

## Meson light-front wavefunctions-applications to $B$ transition form factors

---

**Mohammad Ahmady**<sup>a,\*</sup>

<sup>a</sup>*Department of Physics, Mount Allison University,  
67 York Street, Sackville, New Brunswick, Canada E4L 1E6*

*E-mail:* [mahmady@mta.ca](mailto:mahmady@mta.ca)

The holographic light front wavefunction (HLFWF) for mesons is used to obtain the distribution amplitudes (DA) for light mesons and consequently calculate  $B \rightarrow V$  transition form factors (TFFs), where  $V = \rho, K^*$  and  $\phi$ . The numerical results are extended to high momentum transfer ( $q^2$ ) region using lattice QCD predictions plus two-parameter fits. The TFFs thus predicted by HLFWF are compared with those obtained from QCD Sum Rules.

*21st Conference on Flavor Physics and CP Violation (FPCP 2023)  
29 May - 2 June 2023  
Lyon, France*

---

\*Speaker

## 1. Introduction

Rare B-meson decays are excellent venues for indirect search of new physics beyond the Standard Model (SM). Theoretical predictions of observables in exclusive rare B decays require the knowledge of non-perturbative quantities like TFFs as well as decay constants. Using light-cone sum rules (LCSR) for calculating these TFFs needs the meson Distribution Amplitudes (DAs) as inputs. In most theoretical predictions, DAs used in such calculations are obtained from QCD Sum Rules (QCDSR). In this work, we show the relation between meson DAs and its HLFWF, the latter obtained by solving the holographic Schrödinger Equation for mesons. The differences between our predictions for  $B \rightarrow V$ ,  $V = \rho, K^*$  and  $\phi$  TFFs and those resulted from the QCDSR offers an opportunity to gauge the hadronic uncertainties in these decay modes.

## 2. Light-front wavefunction

In light-front formalism, the hadron state  $|\Psi(P)\rangle$  is the eigenstate of the light-front Hamiltonian, i.e.

$$H_{\text{QCD}}^{\text{LF}}|\Psi(P)\rangle = M^2|\Psi(P)\rangle, \quad (1)$$

where  $H_{\text{QCD}}^{\text{LF}} = P^+P^- - P_{\perp}^2$  is the LF QCD Hamiltonian and  $M$  is the hadron mass. At equal light-front time ( $x^+ = 0$ ) and in the light-front gauge  $A^+ = 0$ , the hadron state  $|\Psi(P)\rangle$  admits a Fock expansion, i.e.

$$|\Psi(P^+, \mathbf{P}_{\perp}, S_z)\rangle = \sum_{n, h_i} \int [dx_i] [d^2\mathbf{k}_{\perp i}] \frac{1}{\sqrt{x_i}} \Psi_n(x_i, \mathbf{k}_{\perp i}, h_i) |n : x_i P^+, x_i \mathbf{P}_{\perp} + \mathbf{k}_{\perp i}, h_i\rangle \quad (2)$$

where  $\Psi_n(x_i, \mathbf{k}_{\perp i}, h_i)$  is the light-front wavefunction (LFWF) of the Fock state with  $n$  constituents and the integration measures are given by

$$[dx_i] \equiv \prod_i^n dx_i \delta(1 - \sum_{j=1}^n x_j) \quad [d^2\mathbf{k}_{\perp i}] \equiv \prod_{i=1}^n \frac{d^2\mathbf{k}_{\perp i}}{2(2\pi)^3} 16\pi^3 \delta^2(\sum_{j=1}^n \mathbf{k}_{\perp j}). \quad (3)$$

$(k_i^+, k_i^-, \mathbf{k}_{\perp i})$  and  $h_i$  are the momentum and helicity of the  $i^{\text{th}}$  constituent and  $x_i = k_i^+/P^+$ . For  $n = 2$ ,

$$\mathbf{k}_{\perp 1} = -\mathbf{k}_{\perp 2} = \mathbf{k}_{\perp},$$

and

$$x_1 = 1 - x_2 = x.$$

The position-space conjugate of  $\mathbf{k}_{\perp}$ , denoted by  $\mathbf{b}_{\perp} = b_{\perp} e^{i\varphi}$ , is the transverse separation between the quark and the antiquark. Introducing a new light-front variable

$$\zeta = \sqrt{x(1-x)} \mathbf{b}_{\perp} = \zeta e^{i\varphi} \quad (4)$$

leads to the meson LFWF in the position-space  $\Psi(\zeta, x, \phi)$  which can be factorized as the following:

$$\Psi(\zeta, x, \phi) \stackrel{\text{factorization}}{=} \frac{\phi(\zeta)}{\sqrt{2\pi\zeta}} e^{iL\phi} X(x) \quad (5)$$

$\phi(\zeta)$  and  $X(x)$  are referred to as the transverse and longitudinal modes and  $L$  is the orbital angular momentum.

### 3. Holographic light-front QCD

When quark masses and quantum loops are neglected, the so-called semi-classical approximation, the transverse mode of the LFWF of a meson satisfies a Schrödinger-like Equation [1]

$$\left( -\frac{d^2}{d\zeta^2} - \frac{1-4L^2}{4\zeta^2} + U_{\text{eff}}(\zeta) \right) \phi(\zeta) = M^2 \phi(\zeta), \quad (6)$$

where  $M$  is the meson mass. This is called the holographic Schrödinger equation because it maps onto the wave equation for string modes propagating in the higher 5-dimensional anti-de Sitter spacetime (AdS<sub>5</sub>). The effective potential in Eq. (6) can be *uniquely* determined from the holographic mapping along with the requirement to introduce a mass scale while preserving the conformal invariance of its underlying action [2]. The result is a quadratic confining potential:

$$U_{\text{eff}}(\zeta) = \kappa^4 \zeta^2 + 2\kappa^2(J-1). \quad (7)$$

$\kappa$  is the emerging confining scale of the transverse mode and  $J = L+S$  is the total angular momentum of the bound state. Once the potential is fixed the eigenvalues and eigenfunctions of the holographic Schrödinger Equation can then be calculated:

$$M^2 = (4n+2L+2)\kappa^2 + 2\kappa^2(J-1) = 4\kappa^2\left(n+L+\frac{S}{2}\right), \quad (8)$$

$$\phi_{n,L}(\zeta) = \kappa^{1+L} \sqrt{\frac{2n!}{(n+L)!}} \zeta^{1/2+L} \exp\left(-\frac{\kappa^2 \zeta^2}{2}\right) L_n^L(x^2 \zeta^2), \quad (9)$$

where  $n$ ,  $L$  and  $S$  are the principal, orbital and spin quantum numbers respectively. As can be seen from Eq. (8), the ground-state, i.e.  $n = L = S = 0$ , is massless, as expected for pions in the chiral limit. On the other hand, the Regge slope for vector mesons determines the fundamental scale of the model:  $\kappa = 0.54$  GeV [3].

The longitudinal mode of the meson HLFWF is obtained by mapping the pion electromagnetic form factors in AdS and in physical spacetime [3]:

$$X(x) = \sqrt{x(1-x)}. \quad (10)$$

### 4. HLFWF and DAs for vector mesons

For the vector mesons (like  $\rho$ ,  $K^*$  and  $\phi$ ), we set  $n = 0$ ,  $L = 0$  and  $S = 1$  in Eq (9) to obtain

$$\Psi_{0,0}(z, \zeta) = X(x)\phi_{0,0}(\zeta) = \frac{\kappa}{\sqrt{\pi}} \sqrt{x(1-x)} \exp\left[-\frac{\kappa^2 \zeta^2}{2}\right], \quad (11)$$

as the HLFWF in the chiral limit. In the presence of the non-zero quark masses, the wavefunction is augmented by an additional exponential factor

$$\Psi_\lambda(z, \zeta) = \mathcal{N}_\lambda \sqrt{x(1-x)} \exp\left[-\frac{\kappa^2 \zeta^2}{2}\right] \exp\left[-\frac{(1-x)m_q^2 + zm_q^2}{2\kappa^2 x(1-x)}\right]. \quad (12)$$

$\lambda$  identifies the polarization of the vector meson.

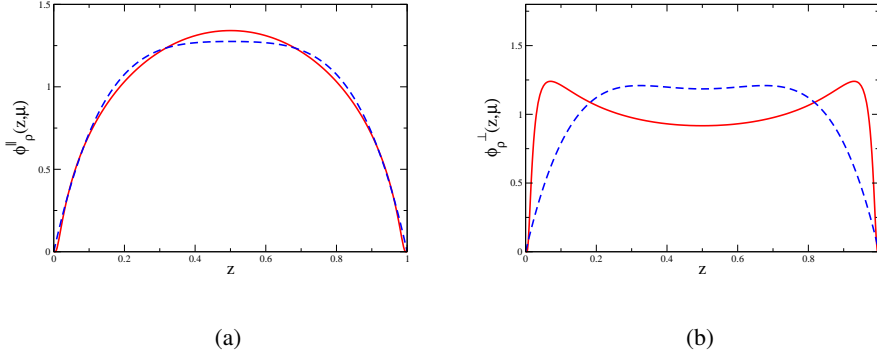


**Figure 1:** Twist-2 DAs for the  $\rho$  meson: (a) longitudinally polarized (b) transversely polarized. Solid Red: Holographic DAs; Dashed Blue: Sum Rules DAs.

Meson DAs can be obtained from its LFWF. For example, the twist-2 holographic DAs for the  $K^*$  meson are then given by

$$\phi_{K^*}^{\parallel}(x, \mu) = \frac{N_c}{\pi f_{K^*} M_{K^*}} \int dr \mu J_1(\mu r) [M_{K^*}^2 x(1-x) + m_{\bar{q}} m_s - \nabla_r^2] \frac{\phi_{K^*}^L(r, x)}{x(1-x)}, \quad (13)$$

$$\phi_{K^*}^{\perp}(x, \mu) = \frac{N_c}{\pi f_{K^*}^{\perp}} \int dr \mu J_1(\mu r) [m_s - x(m_s - m_{\bar{q}})] \frac{\phi_{K^*}^T(r, x)}{x(1-x)}, \quad (14)$$

where  $f_{K^*}$  and  $f_{K^*}^{\perp}$  are the vector and tensor couplings of  $K^*$ . The former can be accessed experimentally through the electronic decay width of the meson and this provides a first constraint for our DAs. In particular, it allows us to constrain the quark masses. Figure (1) shows  $\rho$ -meson DAs obtained from HLFWF compared with those predicted by QCDSR [4]. Similar results for  $K^*$  and  $\phi$  vector mesons can be found in Refs [6, 8]

## 5. $B_{(s)} \rightarrow V$ transition form factors

The hadronic matrix elements are parametrized in terms of nonperturbative TFFs. For example, the 7 TFFs for  $B \rightarrow \rho$  transition are defined in the following equations:

$$\begin{aligned} \langle \rho(k, \varepsilon) | \bar{q} \gamma^{\mu} (1 - \gamma^5) b | B(p) \rangle &= \frac{2iV(q^2)}{m_B + m_{\rho}} \varepsilon^{\mu\nu\rho\sigma} \varepsilon_{\nu}^* k_{\rho} p_{\sigma} - 2m_{\rho} A_0(q^2) \frac{\varepsilon^* \cdot q}{q^2} q^{\mu} \\ &- (m_B + m_{\rho}) A_1(q^2) \left( \varepsilon^{\mu*} - \frac{\varepsilon^* \cdot q q^{\mu}}{q^2} \right) \\ &+ A_2(q^2) \frac{\varepsilon^* \cdot q}{m_B + m_{\rho}} \left[ (p+k)^{\mu} - \frac{m_B^2 - m_{\rho}^2}{q^2} q^{\mu} \right] \end{aligned} \quad (15)$$

$$\begin{aligned} q_{\nu} \langle \rho(k, \varepsilon) | \bar{d} \sigma^{\mu\nu} (1 - \gamma^5) b | B(p) \rangle &= 2T_1(q^2) \varepsilon^{\mu\nu\rho\sigma} \varepsilon_{\nu}^* p_{\rho} k_{\sigma} \\ &- iT_2(q^2) [(\varepsilon^* \cdot q)(p+k)_{\mu} - \varepsilon_{\mu}^* (m_B^2 - m_{\rho}^2)] \\ &- iT_3(q^2) (\varepsilon^* \cdot q) \left[ \frac{q^2}{m_B^2 - m_{\rho}^2} (p+k)_{\mu} - q_{\mu} \right] \end{aligned} \quad (16)$$

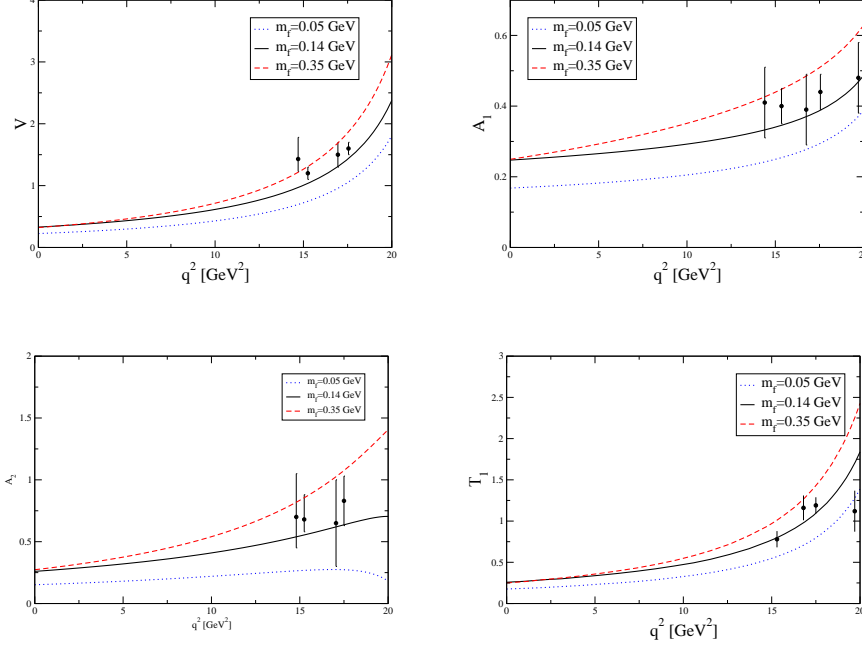


**Figure 2:**  $B \rightarrow \rho$  TFFs predicted by holographic QCD for 3 different quark mass inputs. The points at high  $q^2$  are lattice QCD predictions.

The theoretical calculations of TFFs are mostly based on LCSR which is expected to be accurate at low momentum transfer ( $q^2$ ). Lattice QCD calculations of the TFFs are restricted to high  $q^2$  values for the time being. In this work, DAs obtained from HLFWF are inserted in LCSR to calculate TFFs and extrapolate our predictions to the maximum  $q^2$  value in order to compare to lattice points [7]. Figure (2) illustrates 4 of our predicted  $B \rightarrow \rho$  TFFs for 3 different quark mass values.

Holographic LFQCD predictions for  $B \rightarrow K^*$  TFFs are presented in Refs [8, 9]. In these work, LCSR predictions which are reliable at low  $q^2$  and lattice QCD points at high momentum transfer are combined in two-parameter fits to which are valid for the whole kinematic range of  $q^2$ . Figure (3) shows comparisons between QCDSR and holographic LFQCD calculated as described above for 3 different  $B \rightarrow K^*$  TFFs.

Finally,  $B_s \rightarrow \phi$  TFFs are calculated using  $\phi$  meson DAs obtained from HLFWF and compared with those predicted by QCDSR [6]. The results for 3 TFFs are shown in Figure (4).

## 6. Acknowledgment

MA would like to thank the organizers of FPCP 2019 for the wonderful experience. This work is supported in part by MA and RS's NSERC grants.

## References

- [1] G. F. de Teramond and S. J. Brodsky, Phys. Rev. Lett. **102**, 081601 (2009) doi:10.1103/PhysRevLett.102.081601 [arXiv:0809.4899 [hep-ph]].

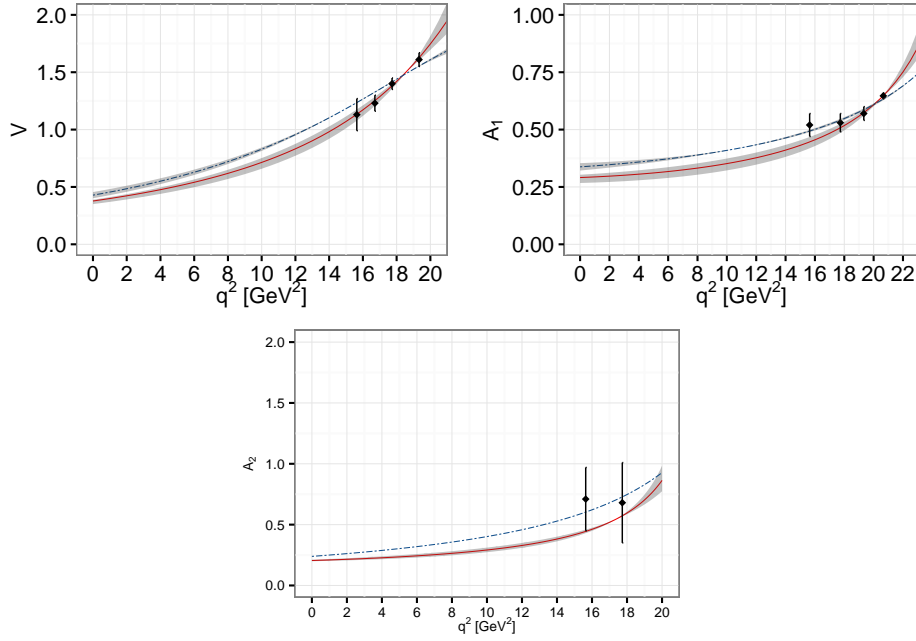


**Figure 3:** Holographic LFQCD predictions for the  $B \rightarrow K^*$  TFFs  $V$ ,  $A_1$ , and  $A_2$ . The two-parameter fits with the available lattice data (red) are shown and compared with the predictions of QCD SR (dashed blue). The shaded band represents the uncertainty in the predicted form factors due to uncertainty bands in DAs and variation in quark masses.

- [2] S. J. Brodsky, G. F. De Téramond and H. G. Dosch, *Phys. Lett. B* **729** (2014), 3-8 doi:10.1016/j.physletb.2013.12.044 [arXiv:1302.4105 [hep-th]].
- [3] S. J. Brodsky, G. F. de Teramond, H. G. Dosch and J. Erlich, *Phys. Rept.* **584**, 1 (2015) doi:10.1016/j.physrep.2015.05.001 [arXiv:1407.8131 [hep-ph]].
- [4] M. Ahmady and R. Sandapen, *Phys. Rev. D* **88**, 014042 (2013) doi:10.1103/PhysRevD.88.014042 [arXiv:1305.1479 [hep-ph]].
- [5] M. Ahmady, R. Campbell, S. Lord and R. Sandapen, *Phys. Rev. D* **89**, no. 7, 074021 (2014) doi:10.1103/PhysRevD.89.074021 [arXiv:1401.6707 [hep-ph]].
- [6] M. Ahmady, S. Keller, M. Thibodeau and R. Sandapen, *Phys. Rev. D* **100** (2019) no.11, 113005 doi:10.1103/PhysRevD.100.113005 [arXiv:1910.06829 [hep-ph]].
- [7] M. Ahmady, R. Campbell, S. Lord and R. Sandapen, *Phys. Rev. D* **88** (2013) no.7, 074031 doi:10.1103/PhysRevD.88.074031 [arXiv:1308.3694 [hep-ph]].
- [8] M. Ahmady, R. Campbell, S. Lord and R. Sandapen, *Phys. Rev. D* **89** (2014) no.7, 074021 doi:10.1103/PhysRevD.89.074021 [arXiv:1401.6707 [hep-ph]].
- [9] M. Ahmady, A. Leger, Z. McIntyre, A. Morrison and R. Sandapen, *Phys. Rev. D* **98**, no. 5, 053002 (2018) doi:10.1103/PhysRevD.98.053002 [arXiv:1805.02940 [hep-ph]].

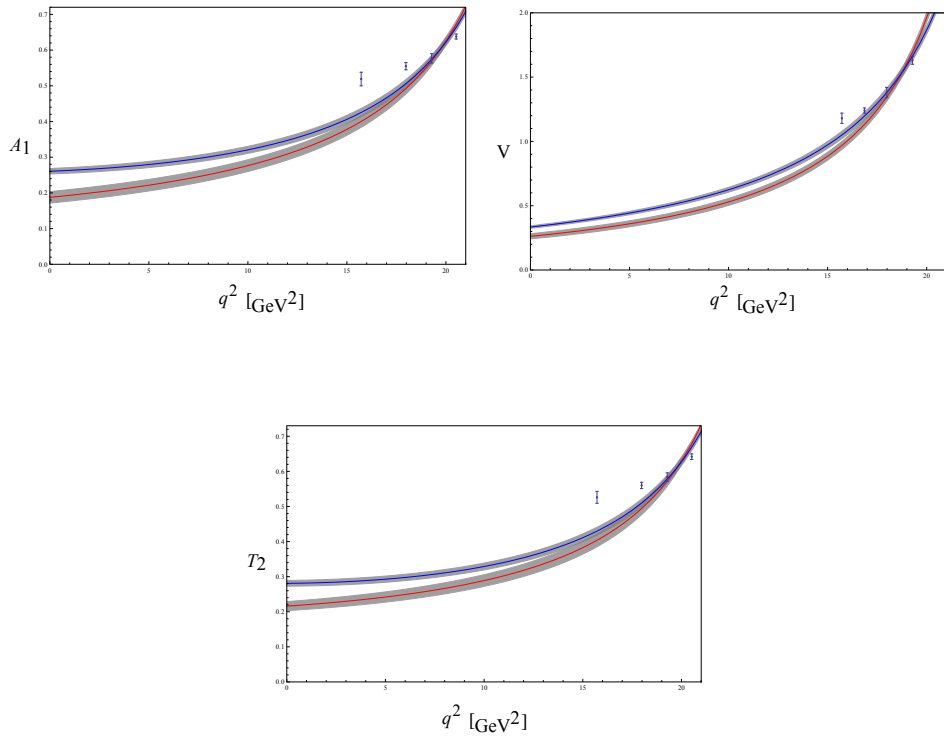


**Figure 4:** Holographic LFQCD predictions for the  $B_s \rightarrow \phi$  TFFs  $A_1$ ,  $V$  and  $T_2$ . The two-parameter fits with the available lattice data (red) are shown and compared with the predictions of QCDSR (dashed blue). The shaded band represents the uncertainty in the predicted form factors due to uncertainty bands in DAs and variation in quark masses.